

## Investigation of non-magnetic impurity doping effect on the MgB<sub>2</sub> superconductor critical temperature

This article has been downloaded from IOPscience. Please scroll down to see the full text article.

2008 J. Phys.: Condens. Matter 20 095212

(<http://iopscience.iop.org/0953-8984/20/9/095212>)

View [the table of contents for this issue](#), or go to the [journal homepage](#) for more

Download details:

IP Address: 129.252.86.83

The article was downloaded on 29/05/2010 at 10:41

Please note that [terms and conditions apply](#).

# Investigation of non-magnetic impurity doping effect on the MgB<sub>2</sub> superconductor critical temperature

Rostam Moradian<sup>1,2,3</sup> and Hamze Mousavi<sup>1</sup>

<sup>1</sup> Physics Department, Faculty of Science, Razi University, Kermanshah, Iran

<sup>2</sup> Nano Science and Technology Research Center, Razi University, Kermanshah, Iran

<sup>3</sup> Computational Physical Science Research Laboratory, Department of Nano-Science, Institute for Studies in Theoretical Physics and Mathematics (IPM), PO Box 19395-5531, Tehran, Iran

Received 4 October 2007, in final form 15 January 2008

Published 14 February 2008

Online at [stacks.iop.org/JPhysCM/20/095212](http://stacks.iop.org/JPhysCM/20/095212)

## Abstract

We have investigated the effect of finite non-magnetic impurity doping concentration on the critical temperature ( $T_c$ ) of the MgB<sub>2</sub> superconductor by using the coherent potential approximation. We found, by choosing the chemical potential  $\mu = -0.47t$  and scattering strength  $\delta = 4.5t$ , that  $T_c$  is reduced with impurity concentration similarly to the measured experimental results.

## 1. Introduction

The discovery of superconductivity with a transition temperature of 39 K in a binary metallic compound of MgB<sub>2</sub> [1] has attracted great interest from scientists all over the world because of its high transition temperature. In the early stage of superconductive material investigation, several inter-metallic material groups including the AlB<sub>2</sub>-type structure were already recognized as candidate materials for ‘high- $T_c$ ’ superconductors, mainly by Matthias and Hulm in the 1950s. ‘Matthias’s rule’ was derived through the investigation of Al<sub>15</sub>-type superconductors [2] such as Nb<sub>3</sub>Sn, V<sub>3</sub>Ga, Nb<sub>3</sub>(AlGe)<sub>2</sub> and Nb<sub>3</sub>Ge<sub>3</sub>, which are important for practical applications. The superconductors discovered in this stage are called ‘BCS superconductors’ because their behavior can be well explained within the framework of the BCS (Bardeen–Cooper–Schrieffer) theory. Most studies performed on this compound indicate that MgB<sub>2</sub> consistently behaves as a phonon-mediated superconductor within the framework of the BCS theory, probably in a strong coupling limit [3, 4]. The transition temperature is surprisingly high for a non-cuprate material, and much above the limit expected for a classical superconducting compound. The observation of a boron isotope effect on  $T_c$  suggests a phonon-mediated pairing mechanism [3]. In the BCS theory [5],  $T_c$  scales with the Debye energy when the effective attractive interaction between electrons is due to phonons.

The effects of impurities in this material are very interesting to study. According to Anderson’s theorem (AT) for classic s-wave superconductors [6–8], non-magnetic impurities

do not affect superconducting properties in zero magnetic field. However, it was shown later by Markowitz and Kadanoff [9] that  $T_c$  is actually reduced in the presence of gap anisotropy and impurity scattering. Also, we have shown [10] that, for low impurity concentrations  $c$  and weak on-site energies, AT is valid, while in the strong scattering limit  $T_c$  is very small even for low  $c$ , and it is completely suppressed by increasing  $c$ ; hence AT is violated in this regime. An application of a two-band model is due to Golubov and Mazin [11]. Indeed, they predicted a rather drastic decrease in  $T_c$  due to inter-band impurity scattering. They also found that, as the inter-band scattering increases, the density of states changes from the two-gap structure inherent in the two-band model to the conventional single-gap structure. This reduction in  $T_c$  has been confirmed recently by a couple of experiments. Wang *et al* [12] measured the specific heat of polycrystalline MgB<sub>2</sub> after irradiation. They found both the suppression of  $T_c$  and a tendency towards a single-gap structure as scattering is increased by irradiation. Lee *et al* [13] clarified the possibility of the complete suppression of superconductivity by replacing B in MgB<sub>2</sub> by C. However, few quantitative calculations have been performed on the impurity effects based on a realistic model for MgB<sub>2</sub> [14]. To study the influence of electron doping on the Mg site in MgB<sub>2</sub>, Slusky *et al* [15] investigated the substitution of Al for Mg to synthesize MgB<sub>1-x</sub>Al<sub>x</sub>B<sub>2</sub> and found that their samples lose superconductivity when  $x$  was near about 0.4. Zhang *et al* [16], Kazakov *et al* [17] and Rogacki *et al* [18] studied the superconductivity of Mg(B<sub>1-x</sub>C<sub>x</sub>)<sub>2</sub> and found that the transition temperature of

their samples decreases when they were doped with carbon powder. We investigated the effects of non-magnetic impurity doping on the reduction in the critical temperature,  $T_c$ , of  $\text{MgB}_2$  superconductor to explain the experimental results of [17, 18]. We calculated  $T_c$  in terms of the impurity doping concentration, in agreement with the experimental data in [17, 18]. In section 2, we introduce the model and obtain the equation of motion. In section 3, by using the coherent potential approximation (CPA), we solve the equation of motion and calculate  $T_c$ . In the last section, we present the numerical results.

## 2. Model and formalism

$\text{MgB}_2$  has the  $\text{AlB}_2$ -type structure. It is composed of two layers of boron and magnesium along the  $c$ -axis in the hexagonal lattice with  $a = 3.08$  and  $c = 3.51$  Å (hexagonal: space group  $P6/mmm$ ). In this structure, the characteristic two-dimensional (2D) honeycomb layers formed by boron atoms are sandwiched by the triangular metal layers, like intercalated graphite. Each Mg atom is at the center of a hexagonal prism of boron atoms at a distance of 2.5 Å. Each boron atom is surrounded by three other boron atoms, forming an equilateral triangle at a distance of  $a_0 = \frac{a}{\sqrt{3}} \sim 1.78$  Å, while the Mg–Mg distance in the plane is equal to the lattice constant  $a$ . Because lattice constants  $a$  and  $c$  in the  $\text{AlB}_2$ -type structure are in the range 3.0–3.2 Å and 3.0–4.0 Å, respectively,  $\text{MgB}_2$  has an intermediate lattice constant among this type of structure. The two electrons belonging to the Mg atom transfer to  $\text{B}_2$ , and the former changes to  $\text{Mg}^{2+}$  while the latter becomes  $\text{B}^{2-}$ . The  $\text{B}_2$  ions become metallic by obtaining two electrons, and Mg ions become insulating by losing two electrons. It has also been shown experimentally by Takahashi *et al* [19] using photoemission spectroscopy that the  $\text{B}_2$  plane is superconducting. Thus we assume that  $\text{MgB}_2$  consists of 2D  $\text{B}_2$  superconductors with weak Cooper pair interaction arranged in parallel planes normal to the direction of the  $c$ -axis.

We start our investigation with the following random extended attractive Hubbard model on a three-dimensional hexagonal lattice,

$$H = - \sum_{ij\sigma\alpha\beta} t_{ij\sigma}^{\alpha\beta} c_{i\sigma}^{\alpha\dagger} c_{j\sigma}^{\beta} + \sum_{ij\sigma\alpha} U_{ij} \hat{n}_{i\sigma}^{\alpha} \hat{n}_{i-\sigma}^{\alpha} + \sum_{i\sigma\alpha} (\varepsilon_i^{\alpha} - \mu) \hat{n}_{i\sigma}^{\alpha}, \quad (1)$$

where  $\alpha$  and  $\beta$  refer to the two non-equivalent sites, A or B, in the graphite-like unit cell (figure 1),  $c_{i\sigma}^{\alpha\dagger}$  ( $c_{i\sigma}^{\alpha}$ ) is the creation (annihilation) operator of an electron with spin  $\sigma$  on Bravais lattice site  $i$ , and  $\hat{n}_{i\sigma}^{\alpha} = c_{i\sigma}^{\alpha\dagger} c_{i\sigma}^{\alpha}$  is the number operator.  $t_{ij\sigma}^{\alpha\beta}$  are the hopping integrals between sites  $i$  and  $j$  with spin  $\sigma$ .  $U_{ij}$  is the attractive interaction potential between electrons of opposite spins at sites  $i$  and  $j$ .  $\mu$  is the chemical potential, and  $\varepsilon_i^{\alpha}$  is the random on-site energy, which takes value 0 with probability  $1 - c$  for host sites (boron host sites) and  $\delta$  with probability  $c$  for impurity sites (related to the carbon impurities).

In the weak interaction regime, for any given configuration of impurity sites the solution of equation (1) is given by the Bogoliubov–de Gennes equation where, for singlet-state superconductors, the order parameter,  $\Delta_{ij}^{\sigma\sigma'} =$

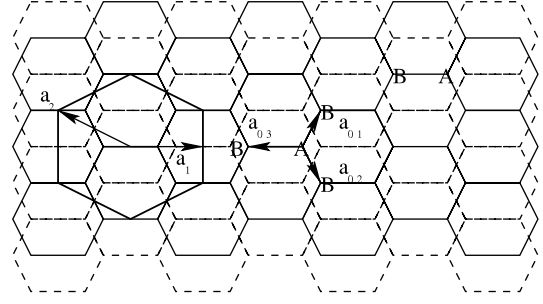


**Figure 1.** A two-dimensional graphite-like ( $\text{B}_2$ ) sheet. The light dashed lines illustrate the Bravais lattice unit cells;  $\mathbf{a}_1$  and  $\mathbf{a}_2$  are the primitive vectors. Each cell includes two non-equivalent sites, which are denoted by A and B.

$\frac{U_{ij}^{\sigma\sigma'}}{\beta} \sum_n G^{\sigma\sigma'}(i, j; i\omega_n)$ , of Cooper pairs with same spins are zero  $\Delta_{ij}^{\uparrow\uparrow} = \Delta_{ij}^{\downarrow\downarrow} = 0$  and  $\Delta_{ij}^{\uparrow\downarrow} = \Delta_{ij}^{\downarrow\uparrow} = \Delta_{ij}$ ,

$$\sum_l \begin{pmatrix} (E + \varepsilon_i + \mu_{i\downarrow})\delta_{il} + t_{il}^{AA} & \Delta_{il} \\ \Delta_{il}^* & (E - \varepsilon_i - \mu_{i\uparrow})\delta_{il} - t_{il}^{AA} \\ t_{il}^{BA} & 0 \\ 0 & -t_{il}^{BA} \\ t_{il}^{AB} & 0 \\ 0 & -t_{il}^{AB} \\ (E + \varepsilon_i + \mu_{i\downarrow})\delta_{il} + t_{il}^{BB} & \Delta_{il} \\ \Delta_{il}^* & (E - \varepsilon_i - \mu_{i\uparrow})\delta_{il} - t_{il}^{BB} \end{pmatrix} \times \mathbf{G}(l, j; E) = \mathbf{I}\delta_{ij}, \quad (2)$$

where  $\mu_{i\sigma} = \mu - U_i n_{i-\sigma}$  is the on-site renormalized chemical potential due to the usual Hartree decoupling,  $\Delta_{il} = \Delta_{il}^0 + \delta\Delta_{il}$  where  $\Delta_{il}^0$  is the clean system order parameter and  $\delta\Delta_{il}$  is the spatial deviation of the order parameter, and  $t_{i\sigma l}^{\alpha\beta}$  is denoted by  $t_{ij}^{\alpha\beta}$ . The coupling parameters  $U_{ij}$  and order parameters  $\Delta_{ij}$  have non-zero values only for two cases:  $U_i^{\parallel}$  and  $\Delta_i^{\parallel}$  if the sites  $i$  and  $j$  coincide in a  $\text{B}_2$  plane, and  $U_{(ij)}^{\perp}$  and  $\Delta_{(ij)}^{\perp}$  if  $i$  and  $j$  are nearest neighbors in adjacent  $\text{B}_2$  planes.  $U_{ij}$  and  $\Delta_{ij}$  defined as,

$$\Delta_{ij} = \Delta_{ij}^{\parallel} + \Delta_{ij}^{\perp}, \quad (3)$$

$$U_{ij} = U_{ij}^{\parallel} + U_{ij}^{\perp}. \quad (4)$$

For first nearest neighbor inter planes, the local order parameter intra plane and local interaction potential intra plane, equations (3) and (4) can be written as,

$$\Delta_{ij} = \Delta_i^{\parallel} \delta_{ij} + \Delta_{(ij)}^{\perp}, \quad (5)$$

$$U_{ij} = U_i^{\parallel} \delta_{ij} + U_{(ij)}^{\perp}. \quad (6)$$

We suppose that these local quantities do not change appreciably on length scales  $\sim \frac{1}{k}$  so, by writing the Fourier transform of order parameters, we have,

$$\Delta^{\perp}(\mathbf{k}) = \frac{1}{N} \sum_{(ij)} \Delta_{(ij)}^{\perp} e^{i\mathbf{k}\cdot\mathbf{r}(ij)} = 2\Delta_{(ij)}^{\perp} \cos(ck_z), \quad (7)$$

$$\Delta^{\parallel}(\mathbf{k}) = \Delta_i^{\parallel}, \quad (8)$$

so we find the gap function in the form,

$$\Delta(\mathbf{k}) = \Delta_i^{\parallel} + 2\Delta_{(ij)}^{\perp} \cos(ck_z). \quad (9)$$

By assuming that the order parameter is real, we obtain,

$$\Delta_i^\parallel = -\frac{U_i^\parallel}{\pi} \int_{-\infty}^{+\infty} dE f(E) \text{Im} G_{12}^{AA\uparrow\downarrow}(i, i; E), \quad (10)$$

$$\Delta_{(ij)}^\perp = -\frac{U_{(ij)}^\perp}{\pi} \int_{-\infty}^{+\infty} dE f(E) \text{Im} G_{12}^{AA\uparrow\downarrow}(i, j; E), \quad (11)$$

and the local band filling,  $n_i$ , is

$$n_i = 2 \int_{-\infty}^{+\infty} dE f(E) \text{Im} G_{11}^{AA\uparrow\uparrow}(i, i; E), \quad (12)$$

where  $f(E) = \frac{1}{e^{\frac{E}{k_B T}} + 1}$ . The Green's function matrix for disordered crystal,  $\mathbf{G}(i, j; E)$ , is defined by,

$$\mathbf{G}(i, j; E) = \begin{pmatrix} G_{11}^{AA\uparrow\uparrow}(i, j; E) & G_{12}^{AA\uparrow\downarrow}(i, j; E) \\ G_{21}^{AA\uparrow\downarrow}(i, j; E) & G_{22}^{AA\uparrow\downarrow}(i, j; E) \\ G_{11}^{BA\uparrow\uparrow}(i, j; E) & G_{12}^{BA\uparrow\downarrow}(i, j; E) \\ G_{21}^{BA\uparrow\downarrow}(i, j; E) & G_{22}^{BA\uparrow\downarrow}(i, j; E) \\ G_{11}^{AB\uparrow\uparrow}(i, j; E) & G_{12}^{AB\uparrow\downarrow}(i, j; E) \\ G_{21}^{AB\uparrow\downarrow}(i, j; E) & G_{22}^{AB\uparrow\downarrow}(i, j; E) \\ G_{11}^{BB\uparrow\uparrow}(i, j; E) & G_{12}^{BB\uparrow\downarrow}(i, j; E) \\ G_{21}^{BB\uparrow\downarrow}(i, j; E) & G_{22}^{BB\uparrow\downarrow}(i, j; E) \end{pmatrix}. \quad (13)$$

Equation (2) can be written as,

$$\mathbf{G}(i, j; E) = \mathbf{G}^0(i, j; E) + \sum_{l\bar{l}} \mathbf{G}^0(i, l; E) \mathbf{V}_{l\bar{l}} \mathbf{G}(l, j; E), \quad (14)$$

where the random potential matrix,  $\mathbf{V}_{l\bar{l}}$ , is defined by,

$$\mathbf{V}_{l\bar{l}} = \begin{pmatrix} \varepsilon_l \delta_{l\bar{l}} - \sum_i U_{l\bar{l}} n_{i\downarrow} & \delta \Delta_l^\parallel \delta_{l\bar{l}} + \delta \Delta_l^\perp \\ \delta \Delta_l^\parallel \delta_{l\bar{l}} + \delta \Delta_l^\perp & -(\varepsilon_l \delta_{l\bar{l}} - \sum_i U_{l\bar{l}} n_{i\uparrow}) \\ 0 & 0 \\ 0 & 0 \\ 0 & 0 \\ \varepsilon_l \delta_{l\bar{l}} - \sum_i U_{l\bar{l}} n_{i\downarrow} & \delta \Delta_l^\parallel \delta_{l\bar{l}} + \delta \Delta_l^\perp \\ \delta \Delta_l^\parallel \delta_{l\bar{l}} + \delta \Delta_l^\perp & -(\varepsilon_l \delta_{l\bar{l}} - \sum_i U_{l\bar{l}} n_{i\uparrow}) \end{pmatrix}, \quad (15)$$

and the clean system Green function,  $\mathbf{G}^0(i, j; E)$ , is given by,

$$\mathbf{G}^0(i, j; E) = \frac{2}{N} \sum_{\mathbf{k}} e^{i\mathbf{k}\cdot\mathbf{r}_{ij}} \times \begin{pmatrix} E + \mu + \epsilon_{\mathbf{k}}^\perp & \Delta^0(\mathbf{k}) & \epsilon_{\mathbf{k}} & 0 \\ \Delta^0(\mathbf{k}) & E - \mu - \epsilon_{\mathbf{k}}^\perp & 0 & -\epsilon_{\mathbf{k}} \\ \epsilon_{\mathbf{k}}^* & 0 & E + \mu + \epsilon_{\mathbf{k}}^\perp & \Delta^0(\mathbf{k}) \\ 0 & -\epsilon_{\mathbf{k}}^* & \Delta^0(\mathbf{k}) & E - \mu - \epsilon_{\mathbf{k}}^\perp \end{pmatrix}^{-1}, \quad (16)$$

where  $\epsilon_{\mathbf{k}} = -\frac{2}{N} \sum_{ij} t_{ij} e^{i\mathbf{k}\cdot\mathbf{r}_{ij}}$  is the band structure and  $\Delta^0(\mathbf{k}) = \Delta^{0\parallel} + \Delta^{0\perp}(\mathbf{k})$  is the Fourier transform of the clean system order parameter. We choose basic vectors as (figure 1),

$$\mathbf{a}_{01} = \frac{a_0}{2} \mathbf{e}_1 - \frac{\sqrt{3}a_0}{2} \mathbf{e}_2, \quad \mathbf{a}_{02} = \frac{a_0}{2} \mathbf{e}_1 + \frac{\sqrt{3}a_0}{2} \mathbf{e}_2, \quad (17)$$

$$\mathbf{a}_{03} = -(\mathbf{a}_{01} + \mathbf{a}_{02}),$$

$$\mathbf{a}_1 = a \mathbf{e}_1, \quad \mathbf{a}_2 = -\frac{\sqrt{3}a}{2} \mathbf{e}_1 + \frac{a}{2} \mathbf{e}_2, \quad \mathbf{a}_3 = c \mathbf{e}_3, \quad (18)$$

where  $a_0 = \frac{a}{\sqrt{3}}$ . In our numerical calculations, hopping to the first nearest neighbors' intra a  $B_2$  plane and inter  $B_2$  planes is considered, and we neglected other hopping terms, so

$$\epsilon_{\mathbf{k}}^{\pm\pm} = \epsilon_{\mathbf{k}}^\pm = \pm t^\parallel \sqrt{1 + 4 \left[ \cos\left(\frac{\sqrt{3}k_x a}{2}\right) + \cos\left(\frac{k_y a}{2}\right) \right] \cos\left(\frac{k_y a}{2}\right)}, \quad (19)$$

$$\epsilon_{\mathbf{k}}^\perp = 2t^\perp \cos(ck_z). \quad (20)$$

Here  $t^\parallel = t_{(ij)}^{AB} = t_{(ij)}^{BA}$  and  $t^\perp = t_{(ij)}^{AA} = t_{(ij)}^{BB}$  are hopping integrals intra a  $B_2$  plane and inter  $B_2$  planes, respectively. Here we do not consider randomness in  $U_{ij}$ , hence the interaction potential is chosen to be  $U_i^\parallel = 2.5t$ , where  $t^\parallel = t = 1.6$  eV and  $t^\perp = 0.96$  eV. Also, for comparison of our results with experimental data, we set the impurity scattering strength,  $\delta = 4.5t$ , and chemical potential,  $\mu = -0.47t$ .

The Dyson equation corresponding to equation (14) for the average Green's function,  $\bar{\mathbf{G}}(i, j; E)$ , is given by,

$$\bar{\mathbf{G}}(i, j; E) = \mathbf{G}^0(i, j; E) + \sum_{l\bar{l}} \mathbf{G}^0(i, l; E) \Sigma(l, l, E) \bar{\mathbf{G}}(l, j; E), \quad (21)$$

where the self-energy,  $\Sigma(l, l, E)$ , is defined by,

$$\sum_l \langle \mathbf{V}_{l\bar{l}} \mathbf{G}(l, j; E) \rangle = \sum_l \Sigma(l, l, E) \bar{\mathbf{G}}(l, j; E). \quad (22)$$

The Fourier transformation of equation (21) leads to the following relation for the average Green's function matrix,  $\bar{\mathbf{G}}(i, j; E)$ :

$$\bar{\mathbf{G}}(i, j; E) = \frac{2}{N} \sum_{\mathbf{k}} e^{i\mathbf{k}\cdot\mathbf{r}_{ij}} \times \begin{pmatrix} E + \mu + \epsilon_{\mathbf{k}}^\perp - \Sigma_{11}(\mathbf{k}, E) & \Delta^0(\mathbf{k}) - \Sigma_{12}(\mathbf{k}, E) \\ \Delta^0(\mathbf{k}) - \Sigma_{21}(\mathbf{k}, E) & E - \mu - \epsilon_{\mathbf{k}}^\perp - \Sigma_{22}(\mathbf{k}, E) \\ \epsilon_{\mathbf{k}}^* & 0 \\ 0 & -\epsilon_{\mathbf{k}}^* \\ \epsilon_{\mathbf{k}} & 0 \\ 0 & -\epsilon_{\mathbf{k}} \\ E + \mu + \epsilon_{\mathbf{k}}^\perp - \Sigma_{33}(\mathbf{k}, E) & \Delta^0(\mathbf{k}) - \Sigma_{34}(\mathbf{k}, E) \\ \Delta^0(\mathbf{k}) - \Sigma_{43}(\mathbf{k}, E) & E - \mu - \epsilon_{\mathbf{k}}^\perp - \Sigma_{44}(\mathbf{k}, E) \end{pmatrix}^{-1}. \quad (23)$$

Equations (10)–(23) should be solved to determine the average Green's function,  $\bar{\mathbf{G}}(i, j; E)$ . In general, there is no analytical solution for such random systems, hence it should be solved approximately. There are many approximations such as the self-consistent Born approximation or Abrikosov–Gorkov theory, which is valid for weak scattering ( $\delta \ll$  bandwidth) and all impurity concentrations [20], the self-consistent T-matrix approximation, which is limited to the case of low impurity concentrations [21], and the coherent potential approximation (CPA), which is valid for all impurity concentrations and impurity strengths [20]. We use the coherent potential approximation (CPA) to obtain the average Green's function matrix,  $\bar{\mathbf{G}}(i, j; E)$ , and  $T_c$ . In the next section, we derive a set of equations for the calculation of  $T_c$  in the CPA formalism.



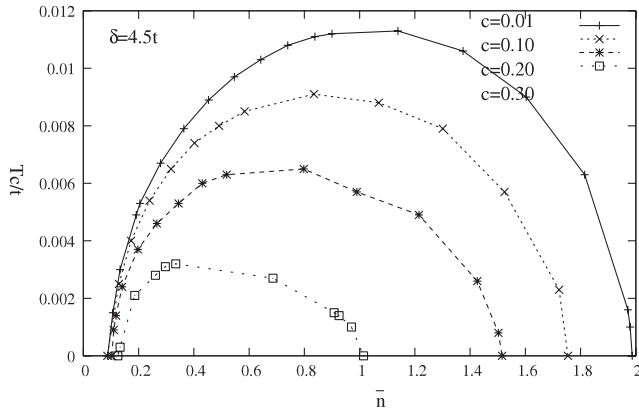


**Figure 2.**  $T_c/t$  in terms of the average band filling,  $\bar{n}$ , for different impurity concentrations,  $c$ , where  $\delta = 4.5t$  bandwidth.

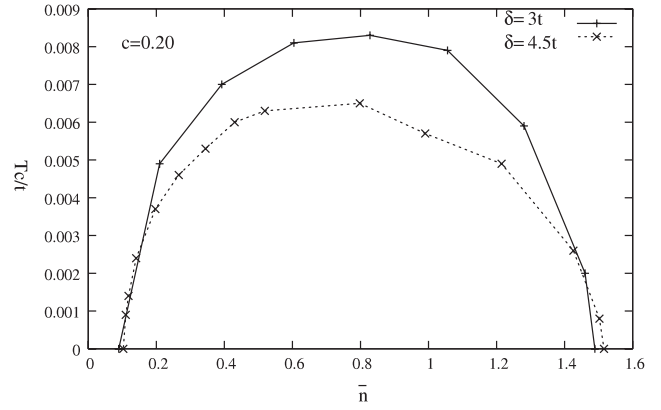


**Figure 4.**  $T_c/t$  in terms of the average band filling,  $\bar{n}$ , for different values of the scattering strength,  $\delta$ .

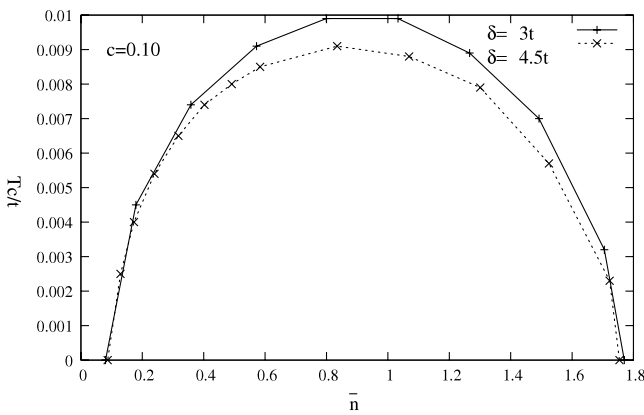


**Figure 3.**  $T_c/t$  in terms of the average band filling,  $\bar{n}$ , for different values of the scattering strength,  $\delta$ .

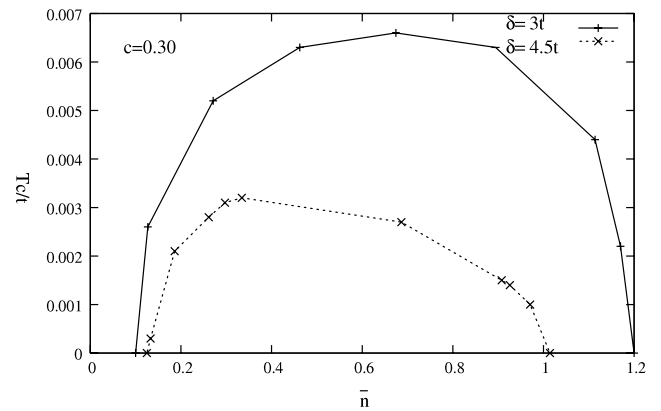


**Figure 5.**  $T_c/t$  in terms of the average band filling,  $\bar{n}$ , for different values of the scattering strength,  $\delta$ .

#### 4. Results and discussions

We have investigated the reduction of the critical temperature,  $T_c$ , of  $\text{MgB}_2$  in terms of non-magnetic impurity doping for different impurity concentrations,  $c$ , and different values of scattering strength,  $\delta$ . To find the role of such impurities on the reduction of  $T_c$ , we have calculated  $T_c$  by varying the impurity concentration  $c$ , impurity strength  $\delta$ , and chemical potential  $\mu$ . Figure 2 illustrates  $T_c/t$  in terms of the average band filling,  $\bar{n}$ , at fixed impurity strength,  $\delta = 4.5t$ , for different impurity concentrations,  $c = 0.01, 0.10, 0.20$  and  $0.30$ , where  $T_c$  is calculated from equation (32); we found that, by increasing the impurity concentration, the critical temperature is reduced and, for some average band filling, there is no superconductivity state. To consider the effect of the scattering strength on  $T_c$ , we have plotted  $T_c/t$  in terms of the average band filling for a fixed impurity concentration and for different scattering strengths.

Figures 3–5 show  $T_c/t$  in terms of the average band filling for a fixed impurity concentration and for different values of the scattering strength,  $\delta = 3t$  and  $\delta = 4.5t$ ; for all these impurity concentrations,  $T_c$  decreased. Figure 6 illustrates that, by increasing the impurity strength and the impurity concentrations,  $T_c$  decreased again. To compare

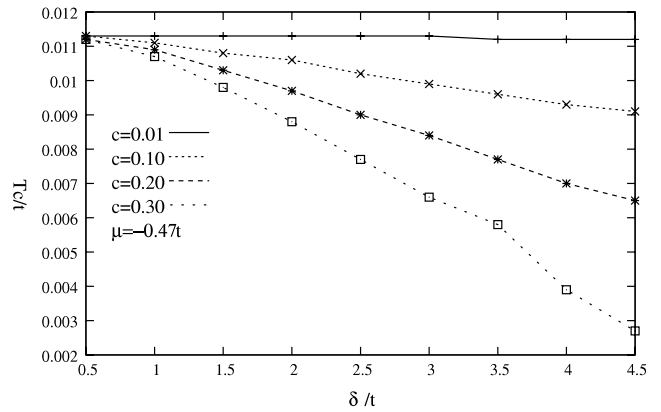


**Figure 6.**  $T_c/t$  in terms of the scattering strength,  $\delta/t$ , for different values of impurity concentrations,  $c$ .

our results with experimental data, we calculated  $T_c$  in terms of the impurity concentration at a fixed impurity strength and also a fixed chemical potential; we found that, just for  $\delta = 4.5t$  and  $\mu = -0.47t$ , our results are in agreement with the reported experimental results [17, 18]. Now we use these parameters,  $\delta = 4.5t$  and  $\mu = -0.47t$ , to calculate  $T_c$  in terms of the impurity concentrations,  $c$ . Figure 7



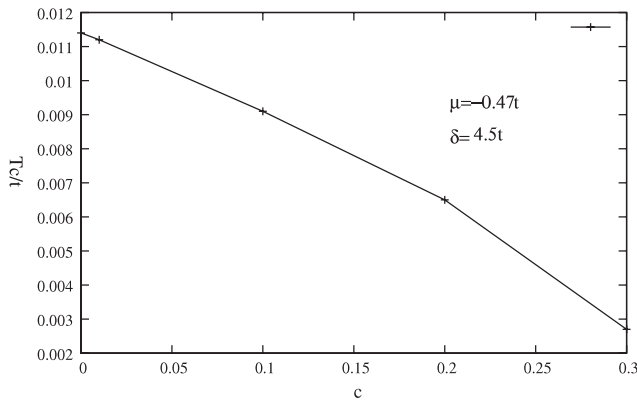


**Figure 7.**  $T_c/t$  in terms of impurity concentrations,  $c$ , where  $\delta = 4.5t$  bandwidth; shown experimentally in [17, 18].

shows  $T_c/t$  in terms of the impurity concentrations for a fixed chemical potential,  $\mu = -0.47t$ , and a fixed impurity strength,  $\delta = 4.5t$ ,  $T_c$  is reduced linearly by increasing the impurity concentration, where it is compatible with the experimental results reported in [17, 18] where they found that the superconducting transition temperature decreases monotonically with increasing carbon content in the full range of substitution that was investigated.

## 5. Conclusion

In conclusion, we have investigated the reduction of the critical temperature  $T_c$  of  $\text{MgB}_2$  superconductor in terms of the non-magnetic impurity doping. Three cases are considered: first, at a fixed scattering strength  $\delta$ ,  $T_c$  is calculated for different impurity concentrations,  $c$ . Second, at fixed impurity concentrations  $c$ ,  $T_c$  is calculated for different scattering strengths,  $\delta$ . Finally, we have investigated the behavior of  $T_c$  in terms of  $c$  for a fixed chemical potential. We found that, by increasing  $\delta$  and  $c$ , the critical temperature decreased and, for some average band fillings, superconductivity disappears. By comparing our results with experimental data, we found that, just for  $\delta = 4.5t$  and  $\mu = -0.47t$ ,  $T_c$  reduces approximately linearly in terms of the impurity concentration,  $c$ .

## References

- [1] Nagamatsu J, Nakagawa N, Murakanaka T, Zenitani Y and Akimitsu J 2001 *Nature* **410** 63
- [2] Matthias B T and Huhl J K 1953 *Phys. Rev.* **89** 439
- [3] Budko S L, Lapertot G, Petrovic C, Cunningham C E, Anderson N and Canfield P C 2001 *Phys. Rev. Lett.* **86** 1877
- [4] Kotegawa H, Ishida K, Kitaoka Y, Muranaka T and Akimitsu J 2001 *Phys. Rev. Lett.* **87** 127001
- [5] Bardeen J, Cooper L N and Schrieffer J R 1957 *Phys. Rev.* **108** 1175
- [6] Anderson P W 1959 *J. Phys. Chem. Solids* **11** 26
- [7] Abrikosov A A and Gorkov L P 1958 *Zh. Eksp. Teor. Fiz.* **35** 1558  
Abrikosov A A and Gorkov L P 1959 *Sov. Phys.—JETP* **8** 1090 (Engl. Transl.)
- [8] Abrikosov A A and Gorkov L P 1959 *Sov. Phys.—JETP* **9** 220
- [9] Markowitz D and Kadanoff L P 1963 *Phys. Rev.* **131** 563
- [10] Moradian R and Mousavi H 2006 *Supercond. Sci. Technol.* **19** 449
- [11] Golubov A A and Mazin I I 1997 *Phys. Rev. B* **55** 15146
- [12] Wang Y, Bouquet F, Sheikin I, Toulemonde P, Revaz B, Eisterer M, Weber H W, Hinderer J and Junod A 2003 *J. Phys.: Condens. Matter* **15** 883
- [13] Lee S, Masui T, Yamamoto A, Uchiyama H and Tajima S 2003 *Physica C* **397** 7
- [14] Mazin I I, Andersen O K, Jepsen O, Dolgov O V, Kortus J, Golubov A A, Kuzmenko A B and van der Marel D 2002 *Phys. Rev. Lett.* **89** 107002
- [15] Slusky J S, Rogado N, Regan K A, Hayward M A, Khalifah P, He T, Inumaru K, Loureiro S M, Haas M K, Zandbergen H W and Cava R J 2001 *Nature* **410** 343
- [16] Zhang S Y, Zhang J, Zhao T Y, Rong C B, Shen B G and Cheng Z H 2001 *Chin. Phys.* **10** 335
- [17] Kazakov S M, Puzniak R, Rogacki K, Mironov A V, Zhigadlo N D, Jun J, Soltmann Ch, Batlogg B and Karpinski J 2005 *Phys. Rev. B* **71** 024533
- [18] Rogacki K, Batlogg B, Karpinski J, Zhigadlo N D, Schuck G, Kazakov S M, Wagli P, Puzniak R, Wisniewski A, Carbone F, Brinkman A and van der Marel D 2006 *Phys. Rev. B* **73** 174520
- [19] Shoma S, Machida Y, Sato T, Takahashi T, Matsui H, Wang S C, Ding H, Kaminski A, Campuzano J C, Sasaki S and Kadowaki K 2003 *Nature* **423** 65
- [20] Moradian R, Annett J F and Gyorffy B L 2000 *Phys. Rev. B* **62** 3508
- [21] Moradian R 2001 *PhD Thesis* Bristol University
- [22] Martin A M, Litak G, Gyorffy B L, Annett J F and Wysokinski K I 1999 *Phys. Rev. B* **60** 7523